DOI: 10.18462/iir.icr.2023.0352

Investigation and analysis of a CO_2 heat pump chiller with novel two-stage evaporator

Jan BENGSCH *[(a)(b)], Mihir Mouchum HAZARIKA[(b)], Armin HAFNER[(b)], Kristina N. WIDELL[(a)]

[(a)] SINTEF Ocean, 7465 Trondheim, Norway , *jan.bengsch@sintef.no, kristina.widell@sintef.no
[(b)] Norwegian University of Science and Technology,
7034 Trondheim, Norway, mihir.m.hazarika@ntnu.no, armin.hafner@ntnu.no
*Corresponding author

ABSTRACT

This study was carried out to investigate the performance of a transcritical CO_2 heat pump chiller that provides heating and cooling simultaneously. There are several applications where such CO_2 systems are implemented, i.e., hotels, commercial kitchens, fishing vessels, etc. Depending on the type of applications, these systems can be designed to achieve the desired hot and cold fluid temperature on the secondary side. The system investigated in the present study is utilized to produce hot water (up to 90°C) and chilled water (4°C). The evaporator utilized for chilled water production is a novel two-stage evaporator. The first stage of this evaporator operates on gravity-fed mode while the second stage operates on ejector-supported mode. The secondary loop is internally connected within the plate heat exchanger. This evaporator configuration gives the possibility to achieve a higher temperature gradient on the secondary fluid side. To analyze the performance of this proposed CO_2 system with the two-stage evaporator, a simulation model was developed in Modelica. Using this model, simulations were carried out to analyze the performance of the system under different operating conditions. Results show that the integration of the two-stage evaporator enhances the overall performance by over 5 % as the cooling capacity is shared equally between the two stages and the suction pressure of the compressor is elevated by utilizing the ejector.

Keywords CO_2, heat-pump chiller, two-stage evaporation, Modelling, Modelica

1. INTRODUCTION

In the course of the energy transition, the European Union (EU) is aiming for climate neutrality across all sectors by the year 2050 (European Commission, 2018). The thermal energy production and consumption has to become more sustainable to achieve that objective. In 2020, only about one-fifth of the heating and cooling demand in the EU was provided by renewable energies and though helped to reduce the greenhouse gas emissions (eurostat, 2020).

One way to provide thermal energy in the form of heat, cold and hot water is to use a heat pump/chiller. If possible, a natural refrigerant such as R-744 should be used to comply with the EU F-Gas Regulation in the long term and to further reduce the greenhouse effect caused by leaking refrigerant. R-744 is non-flammable, non-toxic and does not emit any environmentally harmful emissions during production. Therefore, it has the lowest direct environmental impact of all refrigerants. (Hafner, 2019)

In Scandinavian supermarkets, R-744 refrigeration systems for simultaneous heating and cooling are already state of the art (Gullo et al., 2017a; Gullo et al., 2017b; Karampour and Sawalha, 2018) and with the MultiPACK project (Allouche et al., 2021; Elarga et al., 2021; Gullo et al., 2017a) it should also become state of the art for high performance buildings like hotels and supermarkets independent of the climate conditions. For this to succeed, further adjustments to components of the overall system, such as the evaporator, are necessary to further increase efficiency and adapt operation to warmer climates.

To improve the efficiency of CO_2 evaporators the heat transfer should be carried out with as much liquid contact as possible (Cheng et al., 2008). This can be achieved by using a flooded evaporator which operates without superheating. One possibility to implement flooded evaporators is to use a gravity fed system utilizing the thermosyphon effect. According to Paliwoda (1992), flooded evaporators in the form of gravity fed systems are the most reliable and efficient evaporators in terms of pressure drop and heat transfer (Paliwoda, 1992). Another way to implement flooded evaporators is to use an ejector to ensure the liquid feed (Minetto et al., 2014).

In this study, the integration of a novel two-stage evaporator in a CO_2 heat pump chiller was investigated. This heat-pump chiller is designed to provide simultaneously hot and cold water. In this proposed system, the novel two-stage evaporator was used to produce chilled water. The focus of this work was on the investigation of the new two-stage evaporator. On the one hand, the influence of the distribution of the heat exchanger surface over the two evaporator stages on the system performance was investigated. On the other hand, the part-load behavior of the evaporator was investigated.

2. SYSTEM DESCRIPTION AND MODELLING PROCEDURE

The simulation was performed using the modeling language Modelica, the program Dymola in version 2020x with its standard solver Dassl and the thermal model library TIL/TILMedia (version 3.11.0) from TLK-Thermo GmbH.

2.1. The novel two-stage evaporator

Current heat pump chiller systems are limited by the larger footprint of two heat exchangers and extra piping. Therefore, NTNU, SINTEF and Alfa Laval have worked together to develop a novel two-stage evaporator consisting of two identical brazed plate heat exchangers with 40 plates each. These were assembled back-to-back. What makes this evaporator configuration unique is the integration of a gravity-fed evaporator loop on one side of a plate heat exchanger and an ejector-supported evaporator loop on the other side. The result can be seen in Figure 1 a). A slightly thicker intermediate plate separates the two heat exchangers, which is shown as dashed lines in Figure 1 a) and b). The secondary loop is internally connected within the plate heat exchanger, which significantly reduces the pipework required for two separate heat exchangers. As a result, the compact two-stage heat exchanger requires less space and less connections. This results in a higher capacity per volume of the evaporator and the entire system. Furthermore, the evaporation on two pressure levels and the increase of the suction pressure of the compressor via the ejector is expected to lead to a higher system performance.

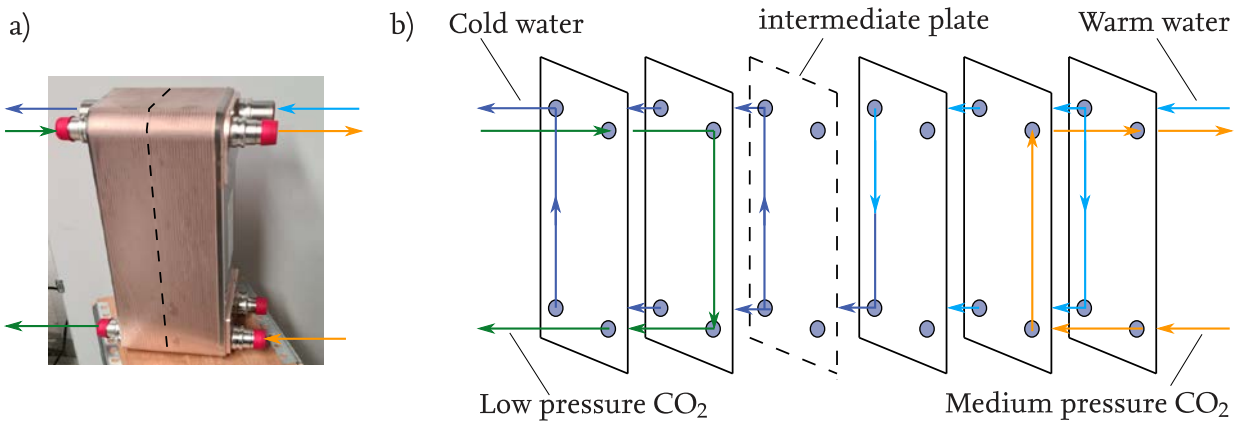

Figure 1 Picture of the novel two-stage evaporator prototype from Alfa Laval a) and simplified sketch of its working principle b)

2.2. Model description

A schematic drawing of the heat pump chiller under consideration is shown in Figure 2. It consists of the two-stage evaporator circuit including separator and expansion valve, an internal heat exchanger (IHX), a compressor, two gas coolers/condensers and an ejector. The changes of state that take place in the heat pump chiller are shown in Figure 3.

Saturated steam is drawn from the separator by the compressor and is superheated by an internal heat exchanger on its way to the compressor inlet. The CO_2 is compressed to high pressure and temperature before being cooled by transferring heat to the secondary fluid in the two gas coolers (GC). As described in Chapter 2.3 below, commercially available HX were used to build the simulation model. Two GCs had to be connected in series to provide sufficient heat transfer surface area. This represents domestic hot water heating and flows in series through both GCs. The CO_2 exiting the second GC is then further cooled by the IHX before entering the ejector as the motive flow. In the ejector, the motive flow is expanded, mixed with the low-pressure suction flow, and then together enter the separator as a medium pressure discharge flow. From the separator, the liquid phase of the refrigerant is fed to the two evaporators. The gravity-fed evaporator is operated on the thermosyphon principle at the medium pressure level of the separator, and the ejector-supported evaporator is operated with the suction mass flow of the ejector at low pressure. Both evaporators are operated without superheating. Using the experimental results presented in Hafner et al. (2022) and the paper by Cheng et al. (2008), the target vapor fraction at the outlet of the evaporators was set at 0.8 for the gravity-fed evaporator and 0.9 for the ejector-supported evaporator. Water flows as a secondary fluid first through the gravity-fed evaporator, where it is precooled, and then through the ejector-supported evaporator, where it is further cooled to the desired temperature.

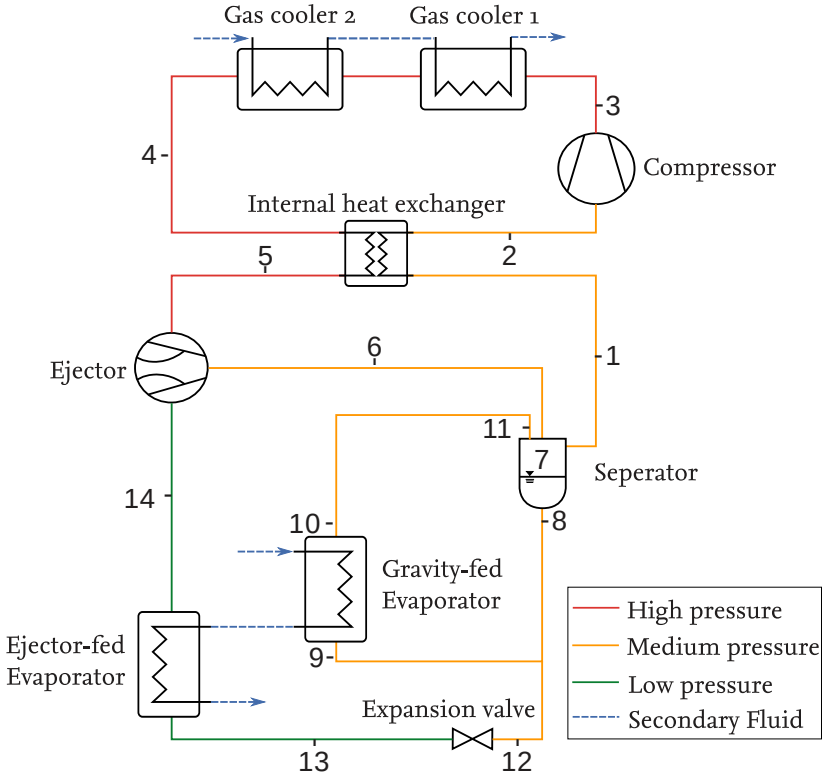

Figure 2 Schematic drawing of the heat pump chiller with two-stage evaporation

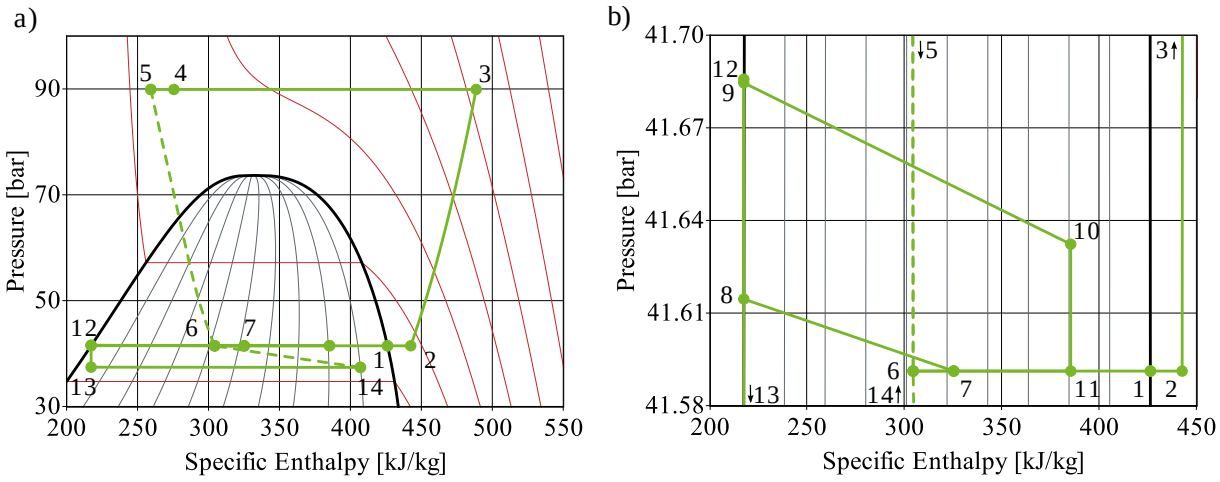

Figure 3 Illustration of the state points under design conditions of a) heat pump chiller in the p, h diagram and b) zoomed in on the state points of the gravity-fed evaporator loop

Table 1 Design conditions for the heat pump chiller (Controlled conditions marked with *)

	Designation	Value	Unit
Geometry Evaporators	Number of plates GFE	40	-
	Number of plates EFE	40	-
	Plate length	0.42	m
	Plate width	0.155	m
Gravity-fed Evaporator	Evaporation pressure	41.68	bar
	Cooling capacity	10.1	kW
	Refrigeration mass flow	3.62	kg/min
	Vapor fraction outlet	80	%
	Water inlet temperature	12	°C
	Water outlet Temperature	8	°C
	Water mass flow	36	kg/min
Ejector-supported Evaporator	Evaporation pressure	37.56	bar
	Cooling capacity	10	kW
	Refrigeration mass flow	3.17	kg/min
	Vapor fraction outlet	90	%
	Water inlet temperature	8	°C
	Water outlet Temperature	4	°C
	Water mass flow	36	kg/min
Motive conditions	High pressure	90	bar
	Motive flow temperature	25	°C
	Ejector efficiency	21	%

2.3. Design conditions of the heat pump chiller

The design of the novel two-stage heat exchanger model for the evaporators is based on the geometry of the prototype provided by Alfa Laval (see Figure 1 a)). It consists of two identical brazed plate heat exchangers. These were assembled back-to-back as a 'sandwich'. The geometry of the evaporators can be found in Table 1. For the remaining heat exchangers, the brazed plate heat exchangers AXP14 from Alfa Laval available on the market are used. For the GCs with 150 plates and for the IHX with 10 plates. Hazarika et al. (2022) described the design and the implementation of the gravity-fed evaporator loop model in detail. It was shown that the gravity-fed evaporator enhanced the system performance and energy efficiency compared to a

system with a dry expansion evaporator. Furthermore, it was shown how important a correct design of the gravity loop is for the system performance. The best results were achieved with a vapor fraction of 0.8 at the outlet of the evaporator. (Hazarika et al., 2022) Hafner et al. (2022) showed the first experimental results of the integrated two-stage evaporator In a heat pump chiller which were used to validate the simulation model. (Hafner et al., 2022)

2.4. Division of the heat transfer area over the two-stages of the evaporator

The prototype of the two-stage evaporator shown in Figure 1 a) consists of two heat exchangers, which are identical and therefore have the same heat exchange surface area. The two-stage evaporator prototype consists of 80 plates, half of which (40 plates) are used for the gravity feed evaporator and the other half for the ejector feed evaporator. For the study, the heat transfer area was varied by distributing the number of plates so that the sum of the two evaporators was always 80 plates. The number of plates in both evaporators varied from a minimum of 5 plates to a maximum of 75 plates per stage. The aim was to determine whether the heat exchanger surface area should be evenly distributed between the two pressure stages, as in the prototype, or whether an uneven distribution of the number of plates would be beneficial to the performance of the system. The coefficient of performance of the refrigeration system (COP_{Ref}) to evaluate the influence of the division of the heat exchanger surface distribution on the system performance was calculated as shown in Eq. (1). This was done by adding the cooling capacities of the gravity-fed evaporator ($\dot{Q}_{GFE}$) and the ejector-supported evaporator ($\dot{Q}_{EFE}$) and then dividing by the shaft power of the compressor (P_{shaft}).

$$COP_{Ref} = \frac{\dot{Q}_{GFE} + \dot{Q}_{EFE}}{P_{shaft}} \qquad \text{Eq. (1)}$$

2.5. Test of part load behavior

Depending on the application, heat pump chillers operate outside their design point for most of the year. Therefore, in addition to the design case, the system behavior at part load is also crucial. Therefore, the cooling load was gradually reduced by half from the design load of 20 kW to 10 kW. This was achieved by increasing the target water outlet temperature in 1 K steps from 4°C (design condition) to 8°C. The COP of the refrigeration system was then calculated as described in Eq. (1) and the load distribution of the cooling load between the two evaporators was considered.

3. RESULTS AND DISCUSSION

3.1. Model Validation

Validation of the simulation model was carried out with measurement data from the test rig. The results are shown in Figure 4 a) for the gravity-fed evaporator and in b) for the ejector-supported evaporator. The two diagrams show the deviations between the experimentally determined cooling capacity (X-axis) and the cooling capacity determined in the simulation (Y-axis). For validation, 12 different operating points were compared. This investigation was performed at an ejector-supported evaporator outlet pressure of 38 bar, at three different water inlet temperatures (12°C, 15°C, and 20°C), and four different water mass flows between 12 kg min−1 to 24 kg min−1. For the gravity-fed evaporator, for which the validation is shown in Figure 4 a), all points are within a deviation of ±15 %. For the validation of the ejector-supported evaporator, which can be seen in part b) of the figure, good agreement was achieved at least for the design temperature of 12°C for all four mass flows. For 15°C, the values deviated slightly more significantly. However, all but one point remained within the ±15 %. At the last operating points with 20°C, only the point of highest water mass flow of 24 kg min−1 was able to stay within the ±15 %. For all other points, the simulated cooling capacity was up to 22 % above the measured one. Despite these deviations, the validation is considered successful

for both evaporators. Further investigation into the differences between the model and reality should be carried out in future studies to determine the cause of the differences.

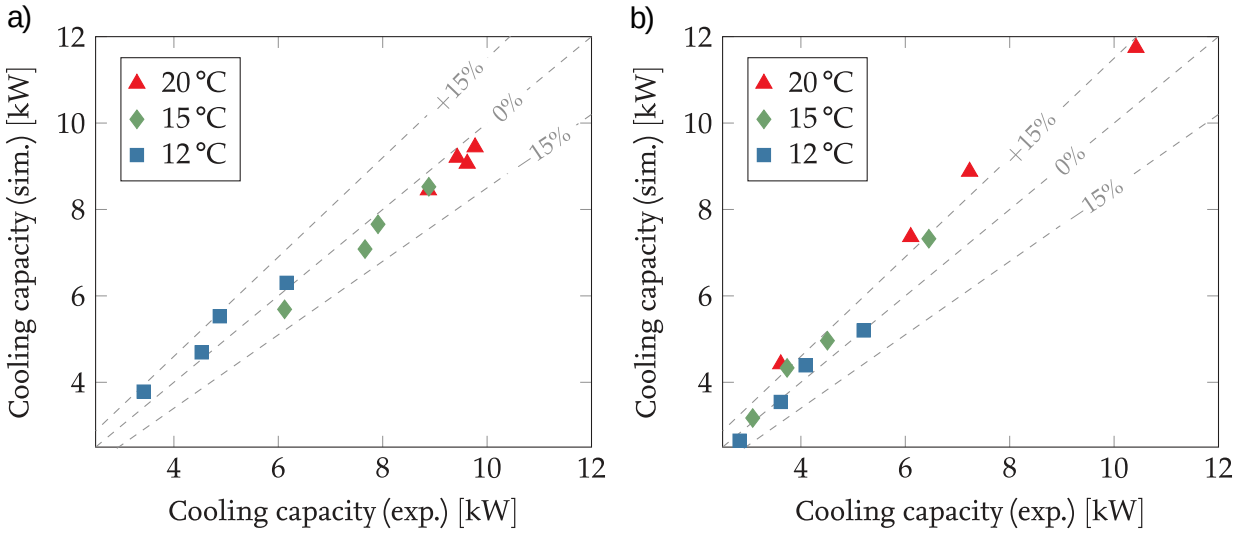

Figure 4 Validation of the two-stage evaporator

3.2. Effect of the division of the number of plates in the two-stage evaporator

The results of the influence of the division of the number of plates on the performance of the two-stage evaporator**.** Figure 5 shows the cooling capacity of both evaporators and the vapor fraction at the outlet of both evaporators versus the number of plates in the gravity-fed evaporator. If only 5 plates are used in the gravity-fed evaporator and 75 in the ejector-supported evaporator, the cooling capacity $\dot{Q}_{EFE}$ is to 75 % on the ejector-supported evaporator. This is equivalent to a cooling capacity of 15 kW. As the number of plates in the gravity-fed evaporator increases, so does the proportion of the cooling capacity. At the same time, the cooling capacity in the ejector-supported evaporator $\dot{Q}_{EFE}$ decreases by the same share that $\dot{Q}_{GFE}$ increases. If the heat exchanger surface is evenly distributed with 40 plates each, there is an inflection point and intersection of the two cooling capacity curves at 10 kW each. With a shift of the plate distribution to the gravity-fed evaporator, $\dot{Q}_{GFE}$ increases to 14 kW at 75 to 5 plates. If the number of plates in the gravity-fed evaporator increases, the vapor fraction x_{GFE} at the outlet of the evaporator also increases. Starting at a vapor fraction of 57 %. With an even distribution of the plates, x_{GFE} reaches the vapor fraction of 80 % targeted in the design. By controlling the expansion valve, the vapor fraction at the outlet of the ejector-supported evaporator remains constant at 90 %.

Furthermore, the influence of the distribution of the number of plates in the evaporators on the coefficient of performance (COP) is considered. This is shown in Figure 6. It shows the COP over the number of plates in the gravity-fed evaporator. As the number of plates in the gravity-fed evaporator increases, the COP also increases to a value of 3.62. This maximum COP takes place with an evenly distributed number of plates. As can be seen in Figure 5, there is a uniform cooling capacity distribution of 10 kW each. At the same time, the temperature difference of the water to be cooled is evenly distributed with 4 K per evaporator.

To better visualize the interaction between the cooling capacity distribution and the relative change of the COP to the maximum COP, this is illustrated in Figure 7. The curve rises steeply up to a cooling capacity distribution $\dot{Q}_{GFE}/\dot{Q}_{EFE}$ of 1:1. At this point, the relative change of the COP to the maximum COP of 3.62 (COP/COP_{max}) is also 1:1. From the curve it can be concluded that an uneven distribution of the cooling load among the evaporators has an unfavorable effect on the system efficiency. This influence is higher with a larger share of the cooling capacity on the gravity-fed evaporator and leads in this investigation to a deviation of the COP from the maximum COP of more than 5 %. This may be since the vapor fraction at this point with 100 % leads to a reduced heat transfer. On the other hand, the separator pressure p_{sep} increases in a similar way as the relative change of the COP. It shows its maximum at a separator pressure of 41.63 bar at a even

cooling load distribution. Since the separator pressure is also the suction pressure of the compressor, low pressures lead to more compressor work and thus to a lower COP.

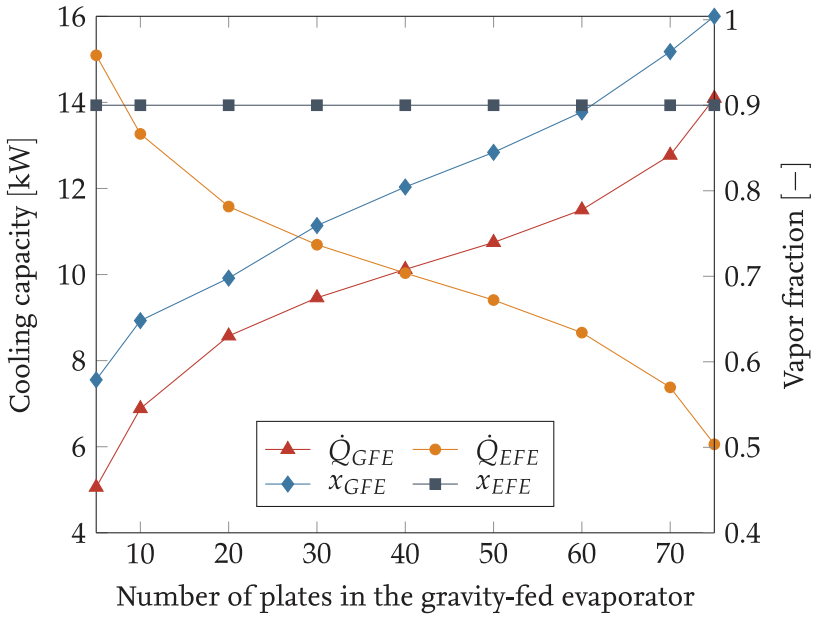

Figure 5 Effect of the division of the number of plates in the two-stage evaporator on the cooling capacity distribution and the vapor fraction in both evaporators.

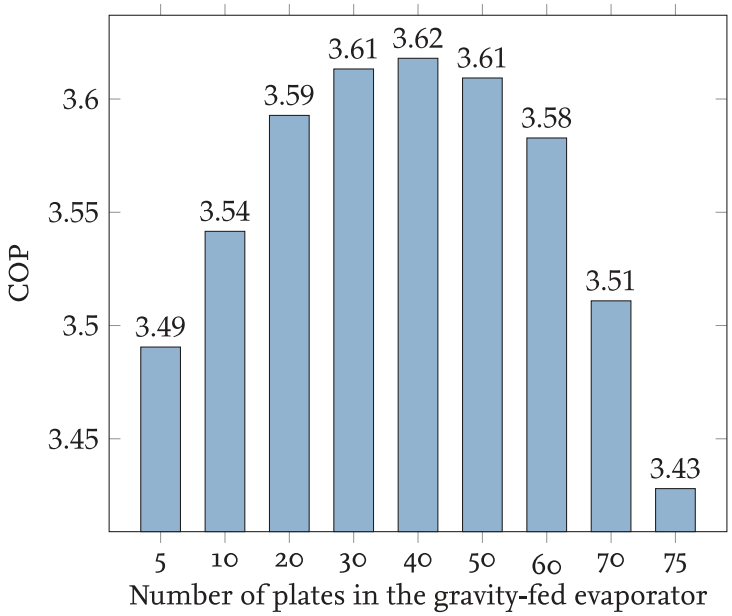

Figure 6 Effect of the division of the number of plates in the two-stage evaporator on the COP.

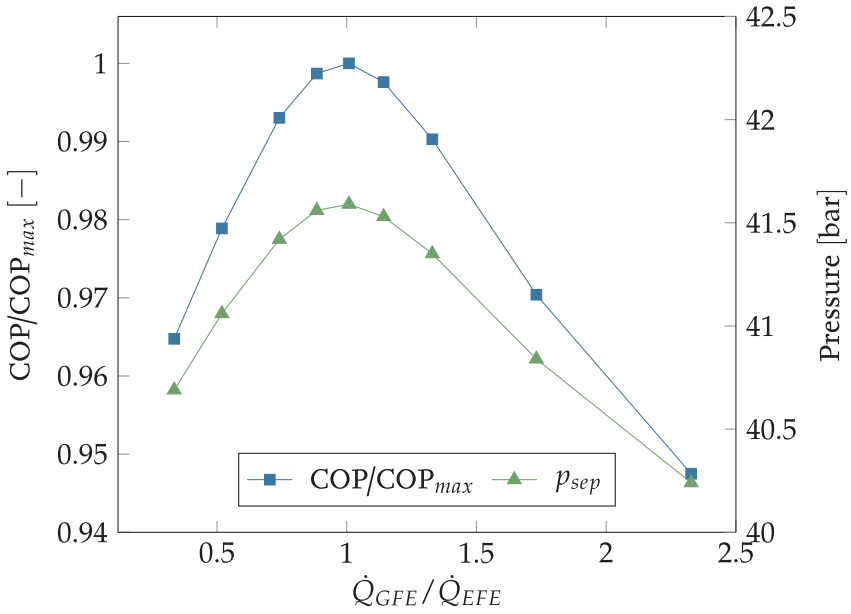

Figure 7 Effect of the division of the number of plates in the two-stage evaporator on the relative change of the COP (COP/COP$_{max}$) and on the separator pressure (p_{sep})

In summary, an even distribution of the heat exchanger surface and thus of the number of plates led to the best results. In this way, the cooling capacities, and the temperature differences of the water to be cooled are equally distributed between the two stages. Another observation is that the pressure lift generated by the ejector is 4 bar for a 40 to 40 split of the number of plates. Under the boundary conditions considered, a cooling of the water from 12°C to 4°C was aimed for. Thereby, the temperature glide was divided equally with 4 K on both evaporators. Since the Δp/ΔT ratio in the two-phase region of CO_2 is approximately 1 bar/K, it can be concluded that the optimum pressure lift to be generated by the ejector is half of the target temperature glide across the two-stage evaporator. This should be investigated in more detail as part of future work.

3.3. Part load behavior of the system

Figure 8 shows the part-load behavior of the two-stage evaporator system based on the cooling capacity distribution and the refrigeration COP over the water outlet temperature of the ejector-supported evaporator. As the outlet water temperature increases, the load distribution shifts further in the direction of the ejector-supported evaporator. At a water outlet temperature of 8°C, almost 65 % of the cooling capacity is provided by the ejector-supported evaporator. The refrigeration COP, on the other hand, increases with the water outlet temperature from 3.62 at design point to 4.03 at half load. This is because the evaporating pressure in both evaporators increases, as can be seen in Figure 9.

Figure 9 shows the two evaporation pressures in the gravity-fed evaporator p_{GFE} and ejector-supported evaporator p_{EFE}. In addition, the vapor fraction at the outlet of the two evaporators x_{GFE} and x_{EFE} over the water outlet temperature of the ejector-supported evaporator is shown. As the outlet water temperature increases, the evaporating pressure in the gravity-fed evaporator also increases. In the ejector-supported evaporator, the pressure increases simultaneously. Thus, the pressure lift of the ejector gradually decreases from 4 bar at full load to 3 bar at the lowest part load investigated. While the vapor fraction at the outlet of the ejector-supported evaporator remains constant at 90 %, the vapor fraction at the outlet of the gravity-fed evaporator decreases from originally 80 % to about 29 %.

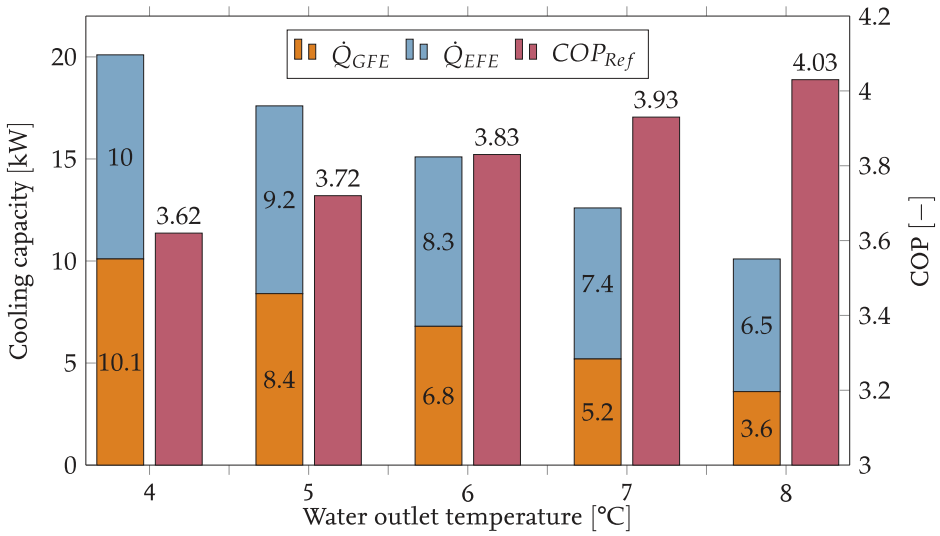

Figure 8 Part load behavior of the two-stage evaporator system based on the cooling capacity distribution and the refrigeration COP

Finally, based on the distribution of the refrigerant mass flow to the gravity-fed evaporator $\dot{m}_{GFE}$ and the ejector-supported evaporator $\dot{m}_{EFE}$ as well as the water-side temperature difference across the two evaporators $\Delta T_{w,GFE}$ and $\Delta T w_{w,EFE}$ over the water outlet temperature of the ejector-supported evaporator, the part-load behavior is shown in Figure 10. As the water outlet temperature increases, the refrigerant mass flow rate $\dot{m}_{GFE}$ flowing through the gravity-fed evaporator increases slightly. In contrast, the refrigerant mass flow rate over the ejector-supported evaporator $\dot{m}_{EFE}$ decreases from an initial 3.17 kg min−1 to 2.17 kg min−1. This is because the expansion valve upstream of the ejector-supported evaporator controls the refrigerant mass flow so that the vapor fraction is constant at 90 %. At the design point, the water temperature differences are both 4 K. Subsequently, both temperature differences decrease at different rates with increasing water outlet temperature. At the highest water outlet temperature, the temperature difference $\Delta T_{w,GFE}$ is 1.42 K and $\Delta T_{w,EFE}$ is 2.58 K.

The investigation of the part-load behavior has shown that the load distribution shifts to the ejector-supported evaporator when the load decreases. At the same time, the COP increases due to the rising evaporating pressure. Since it the results described in chapter 3.2 showed that an even load distribution is the most efficient, further work should investigate the degree to which a constant load distribution is possible even at part load and how this can be implemented.

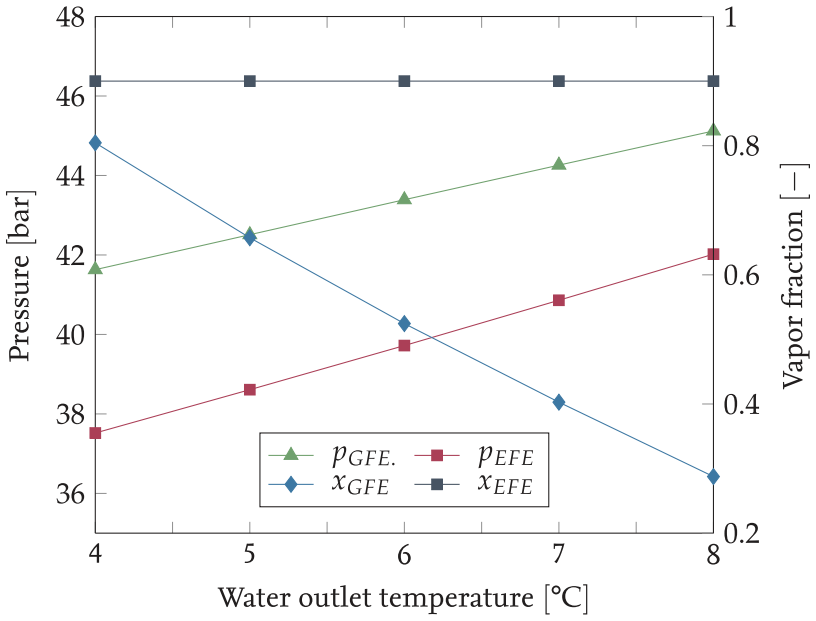

Figure 9 Part load behavior of the two-stage evaporator system based on the evaporating pressure and the vapor fraction at the outlet of the two evaporators

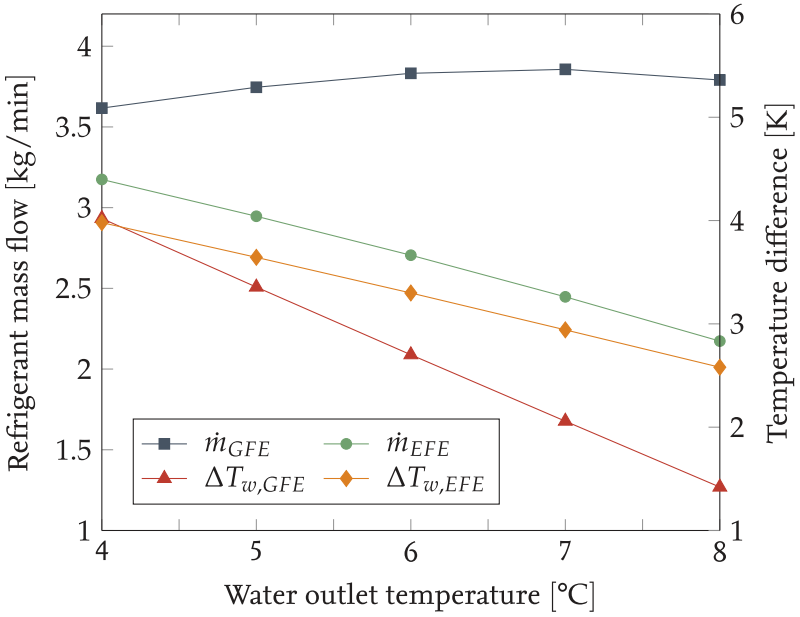

Figure 10 Part load behavior of the two-stage evaporator system based on the distribution of the refrigerant mass flow and the water-side temperature difference

4. CONCLUSION AND FURTHER WORK

In this study, a novel two-stage evaporator was investigated. This was done with simulation models that were created using the TIL library in Dymola/Modelica. Furthermore, the simulation model was validated with measurement data from a test rig. While this validation was considered successful, it also indicated the need for further investigation into the differences between the model and the test rig. When investigating the optimal distribution of the heat exchanger surfaces, it was found that an even distribution of the heat exchanger surface leads to an even distribution of the cooling capacity and thus to a COP increase of more than 5%. With the same distribution of the heat exchanger surfaces, the COP is at a maximum value of 3.62 in this investigation. This is also since with the same distribution, the separator pressure is at its peak, which means that the least amount of compressor work is required. Additionally, it was concluded from the observations that the optimum pressure lift of the ejector should be half of the value of the target

temperature glide of the secondary fluid across both evaporators. Further research should be conducted to verify this conclusion and provide the basis for a simplified and efficient two-stage evaporator design.

Since heat pump chillers are often operated outside the design point, part load behavior was investigated. Compared to the design point, where the load was distributed equally between both evaporators, the load distribution in the part load case was more heavily on the ejector-supported evaporator. At the same time, the COP increases as the load decreases, giving the system good part load performance. However, this is not due to a better distribution of the cooling capacity, but to the increasing evaporating pressure as the water outlet temperature from the evaporator increases. Since the results showed that a uniform load distribution leads to the best results, the following work should investigate if a constant load distribution is also possible at part load.

ACKNOWLEDGEMENTS

The authors gratefully acknowledge the Research Council of Norway and industrial project partners for the financial support for carrying out the present research [NFR project No. 294662, CoolFish].

NOMENCLATURE

IHX	Internal heat exchanger	T	temperature (K)
GC	Gas cooler		
COP	Coefficient of performance	*EFE*	Ejector-supported evaporator
		GFE	Gravity-fed evaporator
$\dot{m}$	Mass flow (kg/s)	*max*	Maximal
$\dot{Q}$	Heat flow (kW)	*Ref*	Refrigeration system
P_{shaft}	Shaft power (kW)	*w*	Water
p	pressure (bar)		

REFERENCES

Allouche, Y., Smitt, S., Hafner, A., 2021. Educational e-book about MultiPACK No 2: Thermal Energy storage integrated into CO2 heat pump systems. NTNU, Trondheim, 16 pp. https://www.ntnu.edu/documents/1272037961/0/723137_Deliverable_16_%28Educational+e-book+about+MULTIPACK+No+2%29.pdf/b544d606-c41e-390f-5be6-c82512af7318?t=1616766385953.

Cheng, L., Ribatski, G., Thome, J.R., 2008. New prediction methods for CO2 evaporation inside tubes: Part II—An updated general flow boiling heat transfer model based on flow patterns. International Journal of Heat and Mass Transfer 51, 125–135. https://doi.org/10.1016/j.ijheatmasstransfer.2007.04.001.

Elarga, H., Sherman, P.K., Hafner, A., 2021. Educational e-book about MultiPACK No 3: CO2 refrigeration and heat pump systems. NTNU, Trondheim, 39 pp. https://www.ntnu.edu/documents/1272037961/0/723137_Deliverable_17_Educational+e-book+about+MULTIPACK+No+3+%283%29.pdf/bdf62beb-47ac-0999-6006-fe067c100fc2?t=1638259340299 (accessed 12 February 2022).

European Commission, 2018. The Commission calls for a climate neutral Europe by 2050*. European Commission. https://ec.europa.eu/clima/news-your-voice/news/commission-calls-climate-neutral-europe-2050-2018-11-28_en (accessed 21 July 2021).

eurostat, 2020. Renewable energy for heating and cooling. Eurostat.

Gullo, P., Fusini, L., Hafner, A., 2017a. Educational e-book about MultiPACK No 1. NTNU, Trondheim, 23 pp. https://www.ntnu.edu/documents/1272037961/0/723137_Deliverable_16_%28Educational+e-book+about+MULTIPACK+No+1%29.pdf/37332fd4-da00-55d8-ab6f-ff7282949ec8?t=1616766346730 (accessed 12 February 2022).

Gullo, P., Tsamos, K., Hafner, A., Ge, Y., Tassou, S.A., 2017b. State-of-the-art technologies for transcritical R744 refrigeration systems – a theoretical assessment of energy advantages for European food retail industry. Energy Procedia 123, 46–53. https://doi.org/10.1016/j.egypro.2017.07.283.

Hafner, A., 2019. The advantages of natural working fluids. https://doi.org/10.18462/IIR.ICR.2019.1030.

Hafner, A., Hazarika, M.M., Lechi, F., Zorzin, A., Pardiñas, Á., Banasiak, K., 2022. Experimental investigation on integrated two-stage evaporators for CO2 heat-pump chillers. 15th IIR-Gustav Lorentzen conference on Natural Refrigerants, 13 June 2022, Trondheim.

Hazarika, M.M., Bengsch, J., Hafsås, J., Hafner, A., Svemdsem, E.S., Ye, Z., 2022. Integration of gravity-fed evaporators in CO2 based heat-pump chillers. https://doi.org/10.18462/iir.gl2022.0091.

Karampour, M., Sawalha, S., 2018. State-of-the-art integrated CO2 refrigeration system for supermarkets: A comparative analysis. International Journal of Refrigeration 86, 239–257. https://doi.org/10.1016/j.ijrefrig.2017.11.006.

Minetto, S., Brignoli, R., Zilio, C., Marinetti, S., 2014. Experimental analysis of a new method for overfeeding multiple evaporators in refrigeration systems. International Journal of Refrigeration 38, 1–9. https://doi.org/10.1016/j.ijrefrig.2013.09.044.

Paliwoda, A., 1992. Calculation of basic parameters for gravity-fed evaporators for refrigeration and heat pump systems. International Journal of Refrigeration 15, 41–47. https://doi.org/10.1016/0140-7007(92)90066-4.